

Identification of Lewis and Blood Group Carbohydrate Epitopes by Ion Mobility-Tandem-Mass Spectrometry Fingerprinting

Johanna Hofmann^{†,‡}, Alexandra Stuckmann[‡], Max Crispin[§], David J. Harvey[§], Kevin Pagel^{†,‡,*} and Weston B. Struwe^{§*}

[†]Fritz Haber Institute of the Max Planck Society, Faradayweg 4-6, 14195 Berlin, Germany.

[‡]Institut für Chemie und Biochemie, Freien Universität Berlin, Takustrasse 3, 14195 Berlin, Germany.

[§]Department of Biochemistry, Glycobiology Institute, University of Oxford, OX1 3QU, United Kingdom

ABSTRACT: Glycans have several elements that contribute to their structural complexity, involving a range of monosaccharide building blocks, configuration of linkages between residues and various degrees of branching on a given structure. Their analysis remains challenging and resolving minor isomeric variants can be difficult, in particular terminal fucosylated Lewis and blood group antigens present on N- and O-glycans. Accurately characterizing these isomeric structures by current techniques is not straightforward and typically requires a combination of methods and/or sample derivatization. Yet the ability to monitor the occurrence of these epitopes is important as structural changes are associated with several human diseases. The use of ion mobility-mass spectrometry (IM-MS), which separates ions in the gas phase based on their size, charge and shape, offers a new potential tool for glycan analysis and recent reports have demonstrated its potential for glycomics. Here we show that Lewis and blood group isomers, which have identical fragmentation spectra, exhibit very distinctive IM drift times and collision cross sections (CCS). We show that IM-MS/MS analysis can rapidly and accurately differentiate epitopes from parotid N-glycans and milk oligosaccharides based on fucosylated fragment ions with characteristic CCSs.

Analysis of glycoconjugates remains a particular challenge in structural biology due to their vast complexity and intricate biosynthesis. Yet the ability to monitor the occurrence of specific carbohydrate markers or changes in protein glycosylation is very important, because they are regularly associated with disease states such as cancer metastasis^{1,2}. This variation in glycosylation is due to cellular changes that affect the non-template driven glycosylation pathway in the endoplasmic reticulum and Golgi apparatus among all nascent glycoproteins. Subtle changes in glycan structures can influence protein function, localization or interactions. These differences arise not only from variations in the number and types of monosaccharide residues, but also from the linkages between them.

One of the most familiar examples of isomeric glycoconjugates are the ABO and Lewis blood group systems. They contain carbohydrate epitopes which consist of a core structure of galactose (Gal) and *N*-acetylglucosamine (GlcNAc) with differently attached fucose (Fuc) residues. These are mediated in individuals by expression of α 1,2-fucosyltransferases and/or α 1,3/4-fucosyltransferases and result in different defined glycan antigens throughout the body. The altered expression of ABO and Lewis glycosyltransferases and changes in glycan structures are commonly associated with cancer formation and regression.³⁻¹¹ The carbohydrate antigen CA19.9, which is specific for sialylated Lewis a (Le^a) epitopes, is the only FDA approved biomarker for pancreatic ductal adenocarcinoma screening, but there are concerns with its use including specificity, levels of detection and non-expression in Le⁻ patients.¹² The ability to discern subtle

changes in fucosylation, which are observed in disease progression and host-pathogen interactions is, therefore, decidedly important but also analytically challenging.

There are several strategies used for characterizing terminal fucose linkages, but each approach has inherent drawbacks and is not always comprehensive. For example, sequential mass spectrometry (MSⁿ) following sample permethylation^{13,14} is highly informative but requires glycan derivatization and is not high-throughput nor as sensitive as HPLC and LC-MS methods.^{15,16} Conversely, HPLC with fluorescence detection requires sequential treatment with numerous exoglycosidase enzymes and the limited availability of linkage-specific fucosidases hinders coverage of these epitopes. Porous graphitized carbon LC-MS² of negative glycan ions can effectively separate isomers and diagnostic fragmentation help pinpoint structures.¹⁷ However, fragmentation data are not always inclusive and, therefore, not all fucose linkages can be resolved, particularly Le^{a/x} and Le^{b/y} structural isomers.¹⁸ An additional complication in the analysis of Lewis antigens is migration and rearrangement of fucose residues along the glycan antennae during collision-induced dissociation (CID) of protonated glycan ions.^{19,20} It was reported that α 1,3-fucose residues migrated to neighbouring Le^x epitopes leading to false identification of Le^y structures but this occurrence was not seen with sodiated glycans which is the focus of this study.

Ion mobility-mass spectrometry (IM-MS) has shown promising results in its capacity to separate isomeric carbohydrates that cannot be resolved by orthogonal methods. To date the use of IM for glycomics has been shown for small oligosaccharides,

intact N-glycans, and glycosaminoglycans.^{21–29} In IM, ions travel through a gas-filled cell aided by an electric field and are separated based on their charge, size, and shape. Gas phase glycan ions adopt distinct structures which allow the separation of isomeric species. In addition, IM drift times can be used to calculate rotationally averaged collision cross sections (CCSs), which are absolute, instrument independent values that can be used for glycan identification.

Here we use IM-MS to differentiate Lewis and blood group epitope isomers, which have identical MS/MS spectra, but display different IM drift times. Furthermore, we take advantage of the ability to generate glycan fragments by CID prior to IM to obtain additional CCS values of fragment ions. This method provides a dual set of m/z and CCS information, which can be used to identify blood group (BG)/Le epitopes by fragmentation of larger glycoconjugates. We demonstrate that this integrated approach can rapidly distinguish BG/Le motifs in milk oligosaccharides and parotid N-glycans without sample derivatization and show that glycans can effectively be identified by their diagnostic fragment CCS fingerprints.

EXPERIMENTAL SECTION

Synthetically derived Lewis and blood group oligosaccharides were purchased from Dextra Laboratories (Reading UK), with the exception of BG-H¹, which was purchased from Elicityl SA (Crolles, France), and diluted with HPLC grade water to a final concentration of 150 μ M prior to use. 1 μ l from the stock solution was added to 8 μ l 1:1 methanol/water (HPLC grade) and 1 μ l 0.1 % formic acid to promote proton adduct formation. Fucosyllacto-N-hexaose (FLNH), difucosyllacto-N-hexaose (DFLNH) and trifucosyllacto-N-hexaose (TFLNH) milk oligosaccharides were purchased from Sigma Chemical Co. Ltd. (Poole, Dorset, UK). Milk oligosaccharides stock solutions were prepared with a concentration of 100 ng/ μ l in water. Prior to analysis, 1 μ l was added to 19 μ l water/methanol (50:50 v/v). Parotid N-glycans were isolated from tissue as previously described.³⁰ N-glycans were released chemically by hydrazinolysis and subsequently re-*N*-acetylated. Sample solutions were stored at -20 °C until analysis.

Ion Mobility-Mass Spectrometry. Traveling wave (TW) IM-MS measurements were performed on a Synapt G2Si instrument (Waters, Manchester, UK). For each analysis 2 μ l of sample were ionized by nano-electrospray ionization (nano-ESI) from gold-coated borosilicate glass capillaries prepared in-house.³¹ Instrument settings were as follows: capillary voltage, 0.8–1.0 kV; sample cone, 100 V; extraction cone, 25 V; cone gas, 40 l/h; source temperature, 150 °C; trap collision voltage, 4–160 V; transfer collision voltage, 4 V; trap DC bias, 35–65 V; IMS wave velocity, 450 m/s; IMS wave height, 40 V; trap gas flow, 2 ml/min; IMS gas flow, 80 ml/min. Data was acquired and processed with MassLynx v4.1 and Driftscope version 2.8 software (Waters, Manchester, UK), and OriginPro 8.5 (OriginLab Corporation, Northampton).

TW-IM-MS and Collision Cross Section Estimation. Arrival time distributions (ATDs) were fit to a single or double Gaussian distribution prior to estimating experimental ^{TW}CCSs. A dextran calibration ladder with known absolute drift tube ^{DT}CCS was used for estimating N-glycan ^{TW}CCS values as previously described.^{32,33} Briefly, measured drift times (t_D) were corrected for m/z dependent delay time from Equation 1 where c is an empirically determined constant ($c = 0.001 \times \text{EDC}$ (enhanced duty cycle) delay coefficient).

$$t'_D = t_D - c\sqrt{m/z} \quad (1)$$

Absolute dextran ^{DT}CCS were corrected for charge (z) and reduced mass (μ) of the ion and the drift gas (Equation 2).

$$\text{CCS}' = {}^{\text{DT}}\text{CCS} / [z \times \left(\frac{1}{\mu}\right)^{\frac{1}{2}}] \quad (2)$$

A linear correlation plot of $\ln(\text{CCS}')$ versus $\ln(t'_D)$ ($R^2 > 0.99$) gives two constants termed the fit-determined constant A and the slope X from the equation:

$$\ln \text{CCS}' = X \times \ln t'_D + \ln A \quad (3)$$

Estimated ^{TW}CCS values can then be determined from experimental drift times by Equation 4, derived from combining Equation 2 and 3 (^{DT}CCS now replaced with ^{TW}CCS):

$${}^{\text{TW}}\text{CCS} = A \times z \times t'^D_X \times \left(\frac{1}{\mu}\right)^{\frac{1}{2}} \quad (4)$$

All TW-IM CCS data are deposited in the GlycoMob database.³⁴ Sample preparation and MS reporting are in accordance with MIRAGE guidelines^{35,36}.

RESULTS AND DISCUSSION

IM-MS of Intact Le and BG Epitope Precursors. The separation potential of individual Lewis and blood group oligosaccharides (Le^a, Le^x, BG-A, BG-H¹, BG-H², Le^b and Le^y) was first tested for intact ions by traveling wave ion mobility (TW-IM) (Figure 1). Le^a, Le^x, BG-H¹ and BG-H² are isomeric trisaccharides consisting of fucose (Fuc), galactose (Gal) and *N*-acetylglucosamine (GlcNAc) residues. BG-A is an isomeric structure which differs in regio- and stereochemistry. Aside from fucose and galactose it additionally contains *N*-acetylgalactosamine (GalNAc) instead of GlcNAc.

Le and BG epitopes are structural similar and contain a core in which Gal and GlcNAc are either connected *via* a β 1 \rightarrow 3 or a β 1 \rightarrow 4 linkage resulting in so-called type 1 and 2 structures,

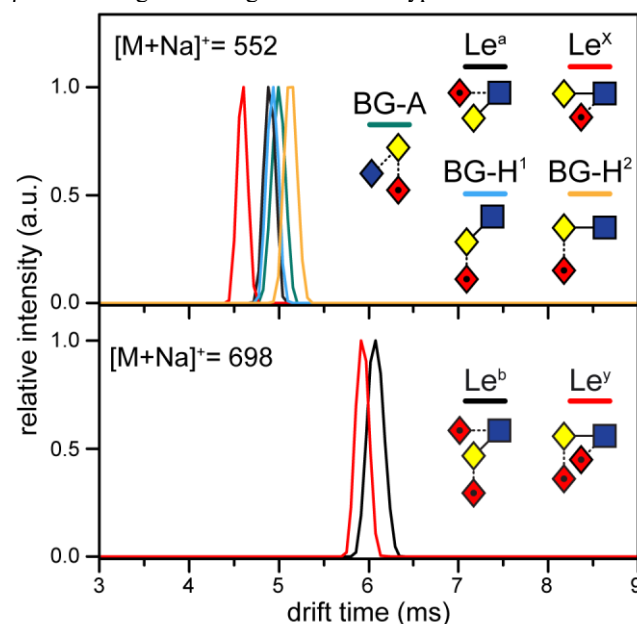


Figure 1. Arrival time distributions (ATDs) of Lewis and blood group oligosaccharides measured as sodium adducts. Trisaccharide isomers Le^a, Le^x, BG-A, BG-H¹, BG-H² (upper panel) and tetrasaccharide isomers Le^b and Le^y are shown (lower panel). Glycan structures are represented using the Oxford system³⁷ (◆=GalNAc, ■=GlcNAc, ◇=Gal, ◆=Fuc).

respectively. The attachment of fucose leads to BG-H structures *via* $\alpha 1 \rightarrow 2$ linkages, Le^x *via* $\alpha 1 \rightarrow 3$ linkages, and Le^a *via* $\alpha 1 \rightarrow 4$ linkages. The exception is the BG-A structure where the fucose is attached as penultimate residue to a GalNAc-Gal core motif. Le^b and Le^y are tetrasaccharide isomers similar to Le^a and Le^x structures, respectively, but containing two fucose residues.

When analysing these structures using IM-MS, different arrival time distributions (ATDs) were observed among sodium adduct ions: for trisaccharides (m/z 552) Le^a (4.90 ms), Le^x (4.59 ms), BG-A (5.00 ms), BG-H¹ (4.93 ms), BG-H² (5.13 ms) and tetrasaccharides (m/z 698) Le^b (6.08 ms) and Le^y (5.93 ms) (Figure 1). Notable is the difference between Le^x and Le^a , which were nearly baseline separated despite minor structural differences (Fuc and Gal linkages are switched). Le^x had a much earlier drift time compared to other trisaccharides and the BG-H¹/BG-H² isomers also differed, but not as much as Le^x/Le^a . Intact tetrasaccharide $[\text{M}+\text{Na}]^+$ adducts could also be differentiated, where the drift time of Le^y (5.93 ms) was shorter than of Le^b (6.08 ms). The observation that both Le^x and Le^y had the lowest drift times implies they adopt more compact gas-phase structures and may correlate with $\alpha 1 \rightarrow 3$ fucose linkages that are present on both ions. Overall the results show that IM can distinguish Le and BG isomers as sodium adduct ions by TW-IM-MS.

IM-MS of Le and BG Epitope Fragment Ions. Next we explored IM separation of fragment ions using a Synapt HDMS instrument that permits CID before and/or after IM separation in the trap or transfer region, respectively (Figure 2). With transfer CID, all fragments are time-aligned with the parent ions while with trap CID, fragments can be resolved according to their CCS. MS/MS of Le and BG $[\text{M}+\text{Na}]^+$ ions resulted primarily in the neutral loss of fucose residues (Le^b/Le^y : m/z 698 \rightarrow 552 \rightarrow 406 and $\text{Le}^a/\text{Le}^x/\text{BG-A}/\text{BG-H}^1/\text{BG-H}^2$: m/z 552 \rightarrow 406) (Figure S-1). These spectra

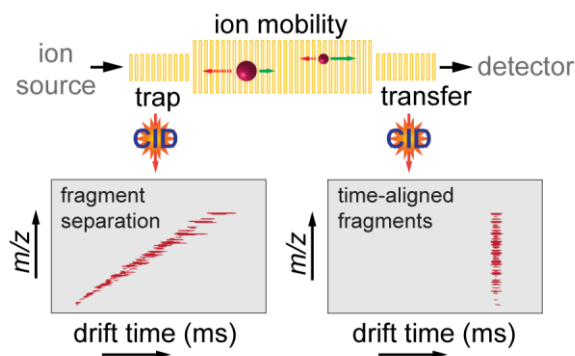


Figure 2. Schematic of a TW-IM-MS instrument depicting IM separation properties of glycan fragment ions for either trap or transfer CID.

were identical, yet the drift times of fragment ions are remarkably different (Figure 3). Most noticeable was Le^y , which yielded four drift peaks from three fragment ions (m/z 698, 552 and 406), with two peaks arising from the m/z 552 fragment. These m/z 552 fragments arise from a $\alpha 1 \rightarrow 2$ fucose or $\alpha 1 \rightarrow 3$ fucose loss and yield fragment structures that are similar to those of the intact Le^x and BG-H² precursors, respectively. As a result, the ATDs of the Le^y m/z 552 fragments (4.61 and 5.12 ms) align very well with the drift times of parent Le^x and BG-H² epitopes. In addition, the drift time of the m/z 406

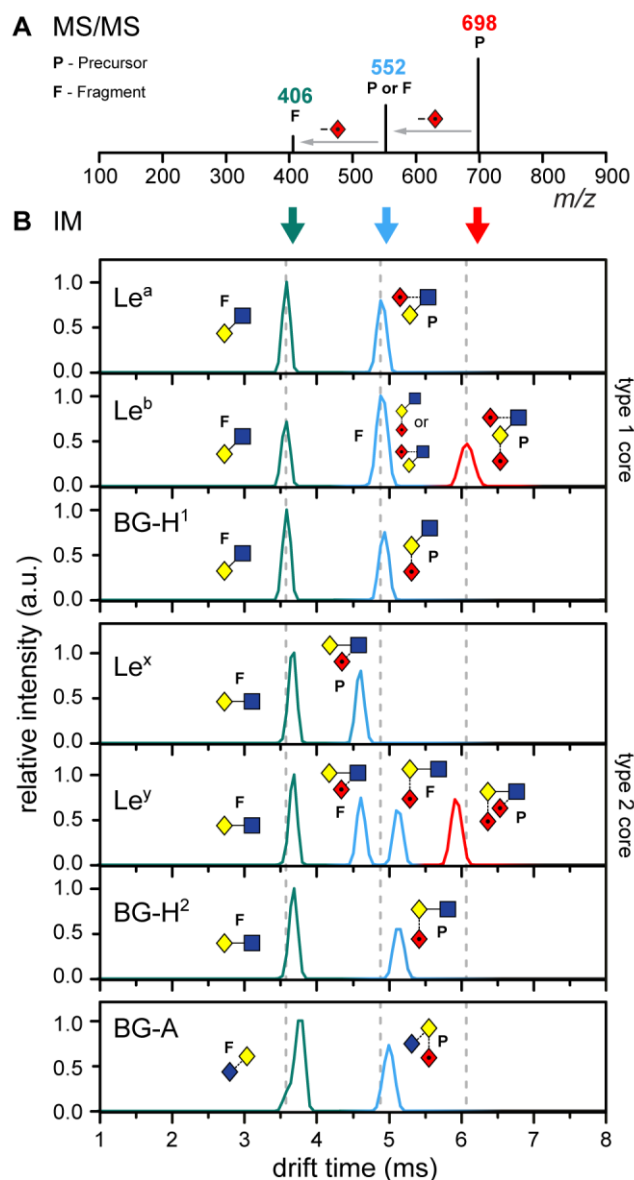
































Figure 3. Tandem MS spectra (A) and IM arrival time distributions (B) of Lewis and blood group precursor and fragment ions as $[\text{M}+\text{Na}]^+$ species. The major fragments resulted from the neutral loss of fucose from the parent ions at m/z 698 and 552.

ion (Gal β 1-4GlcNAc) from Le^y was equal to the m/z 406 fragment from Le^x and BG-H², which is expected as they all correspond to the same type 1 core structure. In contrast to the good separation of fragments arising from Le^y , the IM spectrum of Le^b fragment ions showed only three peaks, one for each MS/MS ion. A single drift peak at 4.96 ms is observed for the m/z 552 fragment, which could be loss of $\alpha 1 \rightarrow 2$ fucose or $\alpha 1 \rightarrow 4$ fucose with fragment structures similar to intact Le^a and BG-H¹ precursors, respectively. This behaviour, however, was expected since the intact Le^a and BG-H¹ trisaccharides had very similar drift times, which did not allow separation. The 552 ATD from Le^b is, therefore, likely to arise from a mixture of both fragment structures (Fuc α 1 \rightarrow 2Gal β 1 \rightarrow 3GlcNAc and Fuc α 1 \rightarrow 4(Gal β 1 \rightarrow 3)GlcNAc). The m/z 406 ions (Gala1 \rightarrow 3GalNAc) that are formed from Le^b , BG-H¹ and Le^a structures on the other hand, all correspond to the same type 2

Table 1. Estimated collision cross sections for the drift gas nitrogen ($^{TW}CCS_{N_2}$) of Lewis and blood group precursor and fragment ions as $[M+Na]^+$ ions. $^{TW}CCS_{N_2}$ values represent the average of three independent measurements and their standard deviation. Fuc-Gal fragments (m/z 349) are not available for Le^a and Le^x structures. Glycan structures are represented using the Oxford system as defined in Figure 1 legend.

	parent and fragment ion $^{TW}CCS_{N_2}$ (Å ²)					
m/z	349	406	534	552	680	698
type	C / *Y	Y	Z / - H ₂ O	Y / intact	- H ₂ O	intact
Le ^a	-	 189 ± 1	 219 ± 2	 223 ± 2		
Le ^b		 190 ± 2	 219 ± 1	 224 ± 1	 252 ± 1	 252 ± 1
BG-H ¹		 188 ± 1	 218 ± 2	 224 ± 1		
Le ^x	-	 191 ± 1	 217 ± 2	 215 ± 2		
Le ^y		 192 ± 2	 218 ± 1	 216 ± 1	 247 ± 1	 248 ± 1
BG-H ²		 191 ± 1	 219 ± 2	 229 ± 2		
BG-A	 177 ± 2	 193 ± 2	 222 ± 2	 225 ± 1		

epitopes and, as a result, exhibit a similar drift time, which is slightly smaller than that observed for type 1 fragments. MS/MS of BG-A also yields a m/z 406 fragment ion, which structurally, however, neither corresponds to those observed for a type 1 nor a type 2 core structure. As a result, the Gal α 1 \rightarrow 3GalNAc fragment from BG-A differed in drift time from both Gal-GlcNAc structures, which underlines that this disaccharide is also diagnostic in IM.

CCSs of Epitope Fragment Ions. The different ATDs of Le and BG parent and fragment ions support IM as a robust method to identify these epitopes. However, analogous to HPLC retention times, ion mobility drift times can vary considerably between instruments/laboratories. To ensure consistent and accurate application of the method it is, therefore, more practical to compare CCSs, which are absolute values for each glycan ion and can be used as standard values for their identification. CCS measurements of sodiated ions were carried out on a TW-IM-MS instrument with nitrogen drift gas ($^{TW}CCS_{N_2}$) using a dextran homopolymer ladder as a calibrant.^{32,38} Le and BG epitopes were measured in triplicate and $^{TW}CCS_{N_2}$ values from all parent/fragment ions are presented in Table 1. The CCS deviation between individual replicates was below 1% and, therefore, well within the error of CCS estimation for oligosaccharides as previously described.^{38,39}

In addition to neutral fucose loss fragments, the CID product ions Fuc-Gal (m/z 349, C-type), Gal-GlcNAc or GalNAc-Gal (m/z 406), and the loss of water from parent ions (-18 Da) were observed. Expectedly the m/z 349 ion was not detected in Le^a and Le^x samples, since they do not have Fuc-Gal linkages. The measured $^{TW}CCS_{N_2}$ values reflected the ATD data shown in Figure 3 and were consistent between experiments, demonstrating

the robustness of the method. CCSs for Le^b and Le^y (m/z 698) were 252 Å² (252 Å² for water loss) and 248 Å² (247 Å² for water loss), respectively. As discussed above, Le^y exhibits two drift peaks at m/z 552 with CCSs of 229 Å² and 216 Å². The Le^y m/z 552 fragments would produce both Le^x and BG-H² structures and correspondingly the CCSs were consistent with those measured for intact Le^x (215 Å²) and BG-H² (229 Å²). Similarly, the Le^b m/z 552 fragment CCS (224 Å²) was identical to the two possible Le^a (223 Å²) and BG-H¹ (224 Å²) precursor CCSs. The CCS values of the m/z 534 ions (water loss from m/z 552) were uniform for all structures (Le^y: 218 Å², Le^b: 219 Å², Le^a: 219 Å², Le^x: 217 Å², BG-H¹: 218 Å², BG-H²: 219 Å²) except for BG-A, which with 222 Å² was considerably larger. Therefore, the m/z 534 B-type fragments are only diagnostic for the BG-A epitope. The Gal-GlcNAc disaccharide (m/z 406) CCSs on the other hand differed and were consistent between β 1 \rightarrow 3 (189 Å²) or β 1 \rightarrow 4 linkages (191 Å²), while the isomer GalNAc α 1 \rightarrow 3Gal (m/z 406) from BG-A had an even larger CCS of 193 Å². Lastly, Fuc α 1 \rightarrow 2Gal fragment ions, which were present on all epitopes, except Le^x/Le^a, were constant with a CCS of 179 Å², but was unexpectedly dissimilar for BG-A (177 Å²). It is unclear why the BG-A Fuc α 1 \rightarrow 2Gal CCS deviates, but it could result from the type of cleavage (*i.e.* Y-type opposed to C-type) or orientation of hydroxyl groups post fragmentation. However, these postulations are difficult to test experimentally. Together the combination of CCSs and MS/MS data are conclusively diagnostic of each epitope and should be considered benchmark values for the sequencing of larger glycan structures by IM-MS/MS.

Epitope Fragments from Milk Oligosaccharides. In order to test if the previously discussed epitope fragment ions are similarly diagnostic for larger structures, the fucosylated milk oligosaccharides FLNH (fucosyllacto-N-hexaose), DFLNH (difucosyllacto-N-hexaose) and TFLNH (trifucosyllacto-N-hexaose) were analysed. All oligosaccharides share the same lacto-N-hexaose (LNH) backbone structure (Gal β 1 \rightarrow 3GlcNAc β 1 \rightarrow 3[Gal β 1 \rightarrow 4GlcNAc β 1 \rightarrow 6]Gal β 1 \rightarrow 4Glc), which is fucosylated to give a Le^x epitope on FLNH, Le^x and BG-H¹ on DFLNH, and Le^x and Le^b on TFLNH.

Importantly, it is known for DFLNH that the primary CID product is the neutral loss of fucose⁴⁰ and we show here that this is also the case for CID of FLNH (Figure 4). However, some fragments of FLNH, DFLNH and TFLNH retain fucose and CCSs could be used to identify individual epitope structures. Le^x is the only fucosylated structure on FLNH and CID produced fucosylated fragments m/z 876 (Gal β 1 \rightarrow 4(Fuc α 1 \rightarrow 3)GlcNAc β 1 \rightarrow 6Gal β 1 \rightarrow 4Glc) and m/z 714 (Gal β 1 \rightarrow 4(Fuc α 1 \rightarrow 3)GlcNAc β 1 \rightarrow 6Gal). The extracted ATDs of each ion gave single peaks (Figure 5). The CCSs of these ions were 279 Å² and 258 Å², respectively. Although the m/z 534 B-type Le^x fragment is present in the MS/MS spectra (Figure 4A), the CCS of this fragment is not diagnostic as discussed above. The m/z 876 ion from DFLNH yielded two ATDs (Figure 5) with CCSs of 279 Å² and 290 Å² (Figure 4B) and can be assigned as Gal β 1 \rightarrow 4(Fuc α 1 \rightarrow 3)GlcNAc β 1 \rightarrow 6Gal β 1 \rightarrow 4Glc (similar to FLNH) and Fuc α 1 \rightarrow 2Gal β 1 \rightarrow 3GlcNAc β 1 \rightarrow 3Gal β 1 \rightarrow 4Glc, which contains the BG-H¹ epitope. There was a single ATD peak for m/z 714 suggesting the presence of the Gal β 1 \rightarrow 4(Fuc α 1 \rightarrow 3)GlcNAc β 1 \rightarrow 6Gal fragment, similar to

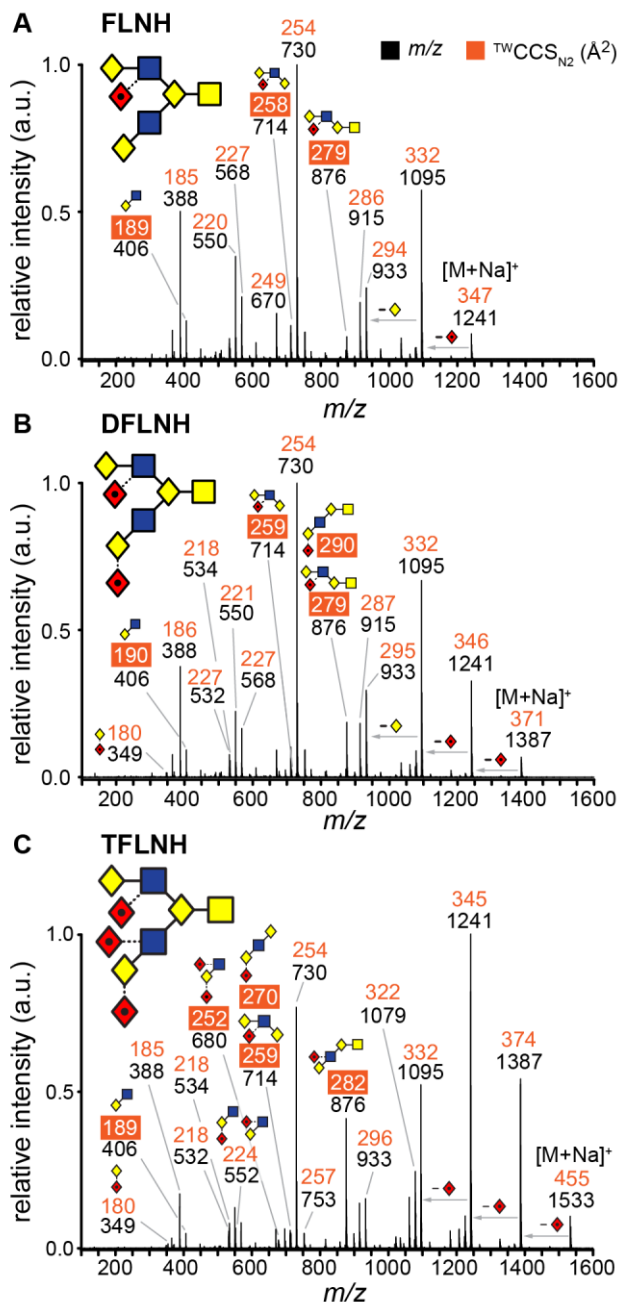


Figure 4. IM-MS/MS of FLNH (A), DFLNH (B) and TFLNH (C) milk oligosaccharides as $[M+Na]^+$ ions. The m/z values (black) with the corresponding $^{TW}CCS_{N_2}$ (orange) are shown. Glycan structures are represented using the Oxford system as defined in the legend to Figure 1. Diagnostic CCSs are highlighted by orange squares.

FLNH, but the presence of (Fucal \rightarrow 2Gal β 1 \rightarrow 3GlcNAc β 1 \rightarrow 3Gal) with the same CCS (259 \AA^2) could not be excluded. However, based on the observation that BG-H¹ and BG-H¹-containing fragments (such as m/z 876 from DFLNH) have greater CCSs than Le^x equivalents, would suggest that the m/z 714 from DFLNH is the Gal β 1-4(Fuca1 \rightarrow 3)GlcNAc β 1 \rightarrow 6Gal structure. Notable for both FLNH and DFLNH was the CCS of the m/z 406 fragment (Gal-GlcNAc, 190 \AA^2), which indicates that this fragment primarily arises from cleavage at the lower antenna leading to a β 1 \rightarrow 3 linked structure.

IM-MS/MS of TFLNH (Figure 4C) supported this hypothesis

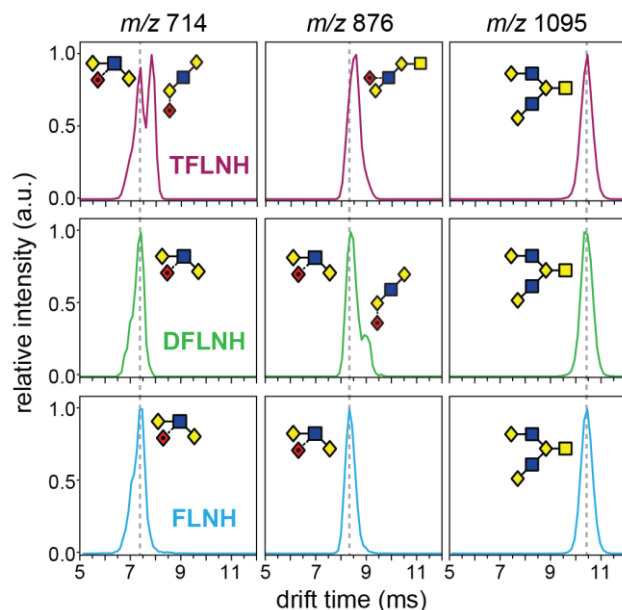


Figure 5. ATDs of diagnostic ions m/z 714, 876 and 1095 from FLNH (blue), DFLNH (green) and TFLNH (purple) milk oligosaccharides. Glycan structures are represented using the Oxford system as defined in the legend to Figure 1.

as demonstrated by the ATD and CCS (282 \AA^2) of the m/z 876 ion which is smaller than the BG-H¹ equivalent (290 \AA^2) yet larger than the Le^x containing ion (279 \AA^2). The CCS of this structure (Gal β 1 \rightarrow 3(Fuca1 \rightarrow 4)GlcNAc β 1 \rightarrow 3Gal β 1 \rightarrow 4Glc) is diagnostic of the Le^a epitope. There was no evidence of the Le^x structure from the m/z 552 fragment, but is detected from the m/z 714 fragment CCS (259 \AA^2), which is similar to that obtained for FLNH. A second peak (270 \AA^2) from m/z 714 was identified (Figure 5) and is the (Fuca1 \rightarrow 2Gal β 1 \rightarrow 3GlcNAc β 1 \rightarrow 3Gal) fragment and again has a greater CCS owing to the presence of BG-H¹. Importantly the m/z 680 ion (252 \AA^2) accurately identifies the Le^b epitope, matching the CCS fragment from the Le^b standard in Table 1. Furthermore the absence of an m/z 552 doublet ATD refutes a Le^y epitope and the measured CCS of 224 \AA^2 indicates the presence of a BG-H¹ or Le^a epitope. Expectedly, the CCS of the Fuca1 \rightarrow 2Gal m/z 349 fragment from DFLNH and TFLNH was 180 \AA^2 and, therefore, consistent with fragments generated from BG-H¹. Finally, the m/z 1095 fragment ATDs from FLNH, DFLNH and TFLNH are equivalent as each oligosaccharide has the same LNH backbone structure. These data are to our knowledge the first example of CCS fragment assignments of milk oligosaccharides, which demonstrate that fucose linkages can be identified by characteristic CCS values of fragment ions.

Epitope Fragments from N-linked Glycans. Lastly, we investigated N-glycans purified from human parotid gland, which are extensively fucosylated and differ among individuals depending on individual sector status.^{18,30,41} N-glycan samples used in this study have previously been characterized primarily as bi- and triantennary structures with up to five fucose residues on the core GlcNAc and the antennae.³⁰ Salivary protein glycosylation is an important factor in pathogen interactions⁴¹, but direct links between glycan structure and susceptibility are debated.^{42,43} Mass spectrometry methods have failed to successfully discriminate Le^{a/x} or Le^{b/y} epitopes

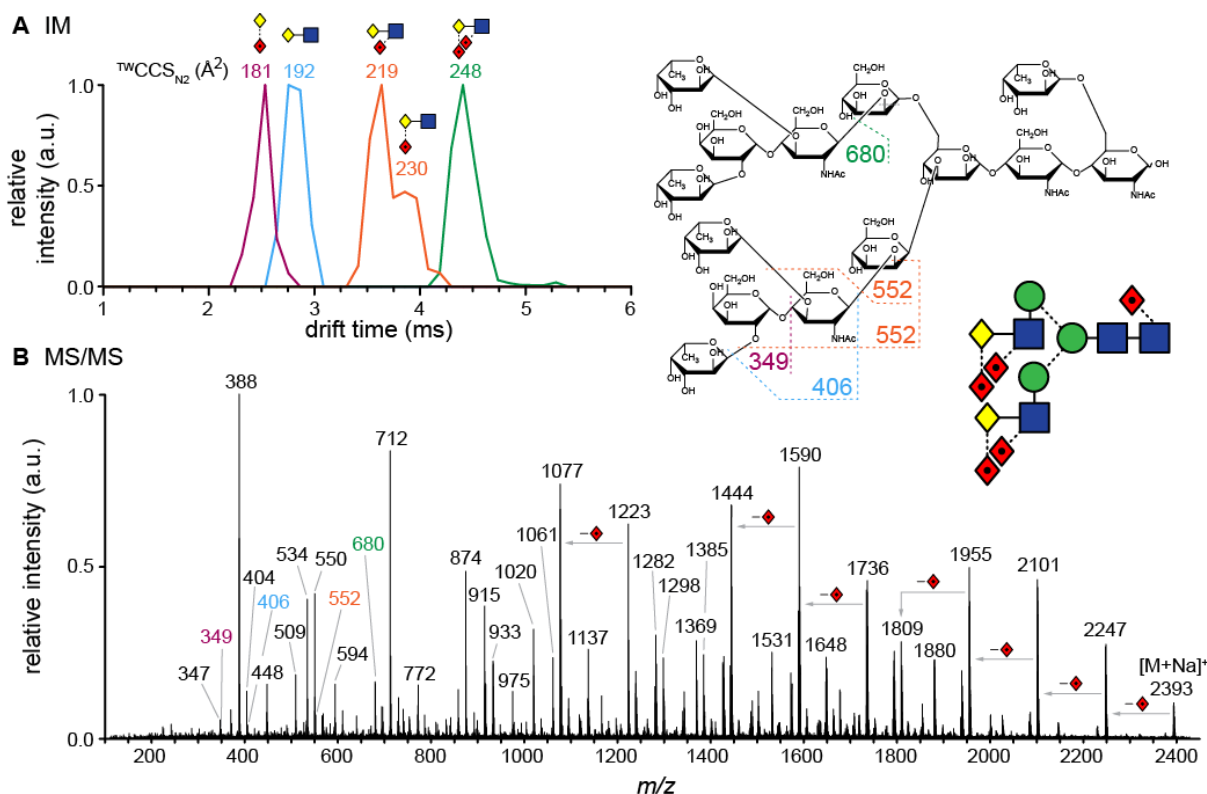


Figure 6. IM-MS/MS of the m/z 2394 $[M+Na]^+$ N-glycan from human parotid gland with A) ATDs and $^{TW}CCS_{N2}$ of diagnostic fragments shown. B) MS/MS spectrum of m/z 2394 with cartoon representation of the known precursor structure. Fragment assignments of the major ions are illustrated. Glycan structures are represented using the Oxford system (■=GlcNAc, ●=Man, ◆=Gal, ◆=Fuc).

on parotid N-glycans^{18,41}, which highlights the need for new approaches to characterize these terminal epitopes.

Tandem MS of the biantennary precursor $Fuc_3Hex_5HexNAc_4$ at m/z 2394 predominantly led to neutral loss fragments at m/z 2248, 2012, 1956, and 1810 (Figure 6). However, also smaller fucosylated fragments were detected and their CCSs could be used to characterize the Le or BG epitope. These include the C-type ions at m/z 349 (Fuc-Hex), 406 (Hex-HexNAc), 552 (Fuc-Hex-HexNAc), and 680 (2Fuc-Hex-HexNAc). The overall composition of the N-glycan suggests four terminal fucose residues and one on the core GlcNAc. Therefore, the m/z 680 fragment is either a Le^b or Le^y fragment, while the m/z 552 ion is a secondary fragment produced from m/z 680 (additional fucose loss), equivalent to those in Figure 3 and Table 1. An ATD with a single feature for m/z 680 and the corresponding CCS (248 \AA^2) are consistent with a Le^y (247 \AA^2) but not a Le^b (252 \AA^2) epitope. More importantly an ATD exhibiting two features was observed for the m/z 552 fragment, which is characteristic for the CID products of Le^y (Figure 3), with CCS values of 219 \AA^2 and 230 \AA^2 , representing the Le^x and BG-H² structures, respectively. The CCS of the Le^x fragment from the parotid N-glycan was slightly larger than that of the individual trisaccharide (215 \AA^2) shown above, which is likely a result of an overlap with a doubly charged species at m/z 550 ($Hex_2HexNAc$ fragment, 220 \AA^2) in the extracted ATD of the m/z 552 fragment. Nonetheless, this observation does not impact the identification of the Le^y structure due to the presence of multiple diagnostic ATD features. Overall, the CCS of m/z 349 identifies $Fuca1 \rightarrow 2Gal$ (181 \AA^2), the m/z 406 fragment is a $Gal\alpha1 \rightarrow 4GlcNAc$ species (192 \AA^2), and taken together with the m/z 680 fragment (Le^y , 248 \AA^2) and the doublet ATD at m/z 552 (Le^x , 219

\AA^2 and BG-H², 230 \AA^2), the presence of Le^y epitopes on both antennae is demonstrated convincingly.

Tandem MS of the $Fuc_2Hex_5HexNAc_4$ ion at m/z 1956 resulted in neutral loss of fucose residues from the parent ion and consequently the m/z 552 C-type fragment was not abundant (Figure S-2). Although the m/z 534 B-type fragment is present, again the CCS of this ion is not diagnostic. However, the absence of the m/z 349 Fuc-Hex ion and the presence of an m/z 406 CCS of 192 \AA^2 suggests a $Gal\alpha1 \rightarrow 4GlcNAc$ linkage and a Le^x structure. This result was expected as the $Gal\beta1 \rightarrow 4(Fuca1 \rightarrow 3)GlcNAc$ structure (Le^x) has been confirmed for this parotid biantennary N-glycan.³⁰ Accordingly, the CCS of the $Gal\beta1 \rightarrow 4(Fuca1 \rightarrow 3)GlcNAc\beta1 \rightarrow 4Man$ fragment (m/z 696, 246 \AA^2) is potentially diagnostic for this epitope. As a final point, IM of complex N-glycans relies on generating ample diagnostic fucosylated CID products and owing to the propensity of fucose loss upon activation, the presence of these ions can be relatively low. Therefore monitoring CID activation energies is critically important for Le and BG identification by IM-MS/MS.

CONCLUSION

Here we demonstrate that IM-MS/MS offers a new technique in glycan analysis by integrating gas-phase separation and CCS values with glycan CID fragmentation. We show that IM of individual Le and BG precursor and fragment ions are decidedly unique and systematically differentiate between isomers. Furthermore, we show that epitopes can be identified in multiply fucosylated parotid gland N-glycans and milk oligosaccharides can be accurately sequenced. These data are significant and the

incorporation of IM with current LC-MS/MS methods will undoubtedly improve glycomics analyses. For example, a similar approach revealed that $\alpha 2 \rightarrow 3$ and $\alpha 2 \rightarrow 6$ N-acetylneuraminic acid linkages can be differentiated by examining oxonium $[M+H]^+$ fragments from glycopeptide precursor ions.^{23,44}

There is sufficient and growing evidence that glycan isomers adopt distinct gas-phase structures allowing for separation and identification of previously indistinguishable structures^{22,28,45,46}. To date the majority of IM studies for glycomics have focused on intact molecular ions, particularly for N-glycans. Here we demonstrate that highly informative structural information lies beneath MS/MS fragmentation spectra when IM is explored. Together, these data can differentiate complex terminal fucose epitopes that have persistently challenged glycomics analyses. MS analysis of sodiated N-glycans is typically less popular owing to the scarcity of informative cross-ring fragments compared to negative ion analysis. On the other hand, analysis of negative ions for IM sequencing of glycoconjugates is less favourable compared to positive ions, because glycans ionize more efficiently as cation metal complexes⁴⁷, readily form sodium adducts, and, most importantly, yield B- and C-type fucosylated fragments that can be compared to corresponding Le and BG ion CCS values.

Lastly, there are potential complications that would be resolved by incorporating LC prior to MS/MS and IM. Specifically, the presence of isomeric molecular ions would be difficult to resolve through a direct infusion ESI approach as the MS/MS spectrum would include data from multiple glycan structures. A 2-dimensional separation analysis by LC-IM-MS/MS has tremendous potential for glycomics and the data presented here establishes that IM information from fragment ions is exceedingly informative and provides a unique fingerprint that can assign unknown fucosylated epitopes from complex glycan mixtures. With the continued development of the method comes a tremendous need for software tools to calculate CCS values and since CCSs are absolute values, the sharing of datasets in the form of curated databases, such as GlycoMob³⁴, is essential for continued success of ion mobility for glycomics.

ASSOCIATED CONTENT

Supporting Information

The Supporting Information Available: MS/MS spectra of synthetic epitopes (Figures S-1) and IM-MS data of the N-glycan from human parotid gland (Figure S-2). This material is available free of charge via the Internet at <http://pubs.acs.org>.

AUTHOR INFORMATION

Corresponding Author

* weston.struwe@bioch.ox.ac.uk (WBS) & kevin.pagel@fu-berlin.de (KP) Fax: +44 (0)1865 285445 (WBS) & +49 30 838472703 (KP)

Author Contributions

The manuscript was written through contributions of all authors. All authors have given approval to the final version of the manuscript.

ACKNOWLEDGMENT

W.S. and M.C. gratefully acknowledges a research grant from Against Breast Cancer (www.againstbreastcancer.org); UK Charity

1121258). M.C. is the Against Breast Cancer Fellow in Cancer Therapeutics at Oriel College, Oxford.

REFERENCES

- (1) Takada, A.; Ohmori, K.; Yoneda, T.; Tsuyuoka, K.; Hasegawa, A.; Kiso, M.; Kannagi, R. *Cancer Res.* **1993**, *53*, 354-361.
- (2) Sozzani, P.; Arisio, R.; Porpiglia, M.; Benedetto, C. *Int. J. Surg. Pathol.* **2008**, *16*, 365-374.
- (3) Engel, P.; Dabelsteen, E.; Francis, D.; Graem, N. *APMIS* **1996**, *104*, 741-749.
- (4) Itzkowitz, S. H.; Yuan, M.; Ferrell, L. D.; Ratcliffe, R. M.; Chung, Y. S.; Satake, K.; Umeyama, K.; Jones, R. T.; Kim, Y. S. *J. Natl. Cancer Inst.* **1987**, *79*, 425-434.
- (5) Kim, Y. S.; Itzkowitz, S. H.; Yuan, M.; Chung, Y.; Satake, K.; Umeyama, K.; Hakomori, S. *Cancer Res.* **1988**, *48*, 475-482.
- (6) Le Pendu, J.; Marionneau, S.; Cailleau-Thomas, A.; Rocher, J.; Le Moullac-Vaidye, B.; Clement, M. *APMIS* **2001**, *109*, 9-31.
- (7) Myers, R. B.; Srivastava, S.; Grizzle, W. E. *J. Urol.* **1995**, *153*, 1572-1574.
- (8) Ogawa, J.; Sano, A.; Inoue, H.; Koide, S. *Ann. Thorac. Surg.* **1995**, *59*, 412-415.
- (9) Schuessler, M. H.; Pintado, S.; Welt, S.; Real, F. X.; Xu, M.; Melamed, M. R.; Lloyd, K. O.; Oettgen, H. F. *Int. J. Cancer* **1991**, *47*, 180-187.
- (10) Xie, X.; Boysen, M.; Clausen, O. P.; Bryne, M. A. *Laryngoscope* **1999**, *109*, 1474-1480.
- (11) Yin, B. W.; Finstad, C. L.; Kitamura, K.; Federici, M. G.; Welshinger, M.; Kudryashov, V.; Hoskins, W. J.; Welt, S.; Lloyd, K. O. *Int. J. Cancer* **1996**, *65*, 406-412.
- (12) Misk, D. E.; Patwa, T. H.; Lubman, D. M.; Simeone, D. M. *J. Natl. Compr. Canc. Netw.* **2007**, *5*, 1034-1041.
- (13) Ashline, D. J.; Hanneman, A. J.; Zhang, H.; Reinhold, V. N. *J. Am. Soc. Mass Spectrom.* **2014**, *25*, 444-453.
- (14) Reinhold, V.; Zhang, H.; Hanneman, A.; Ashline, D. *Mol. Cell. Proteomics* **2013**, *12*, 866-873.
- (15) Jensen, P. H.; Karlsson, N. G.; Kolarich, D.; Packer, N. H. *Nat. Protoc.* **2012**, *7*, 1299-1310.
- (16) Stockmann, H.; O'Flaherty, R.; Adamczyk, B.; Saldova, R.; Rudd, P. M. *Integr. Biol.* **2015**, *7*, 1026-1032.
- (17) Karlsson, N. G.; Schulz, B. L.; Packer, N. H. *J. Am. Soc. Mass Spectrom.* **2004**, *15*, 659-672.
- (18) Everest-Dass, A. V.; Jin, D.; Thaysen-Andersen, M.; Nevalainen, H.; Kolarich, D.; Packer, N. H. *Glycobiology* **2012**, *22*, 1465-1479.
- (19) Wuhler, M.; Koeleman, C. A.; Hokke, C. H.; Deelder, A. M. *Rapid Commun. Mass Spectrom.* **2006**, *20*, 1747-1754.
- (20) Harvey, D. J.; Mattu, T. S.; Wormald, M. R.; Royle, L.; Dwek, R. A.; Rudd, P. M. *Anal. Chem.* **2002**, *74*, 734-740.
- (21) Huang, Y.; Dodds, E. D. *Anal. Chem.* **2013**, *85*, 9728-9735.
- (22) Hofmann, J.; Hahm, H. S.; Seeberger, P. H.; Pagel, K. *Nature* **2015**, *526*, 241-244.
- (23) Hinneburg, H.; Hofmann, J.; Struwe, W. B.; Thader, A.; Altmann, F.; Varon Silva, D.; Seeberger, P. H.; Pagel, K.; Kolarich, D. *Chem. Commun.* **2016**, *52*, 4381-4384.
- (24) Gray, C. J.; Thomas, B.; Upton, R.; Migas, L. G.; Eysers, C. E.; Barran, P. E.; Flitsch, S. L. *Biochim. Biophys. Acta* **2016**, *1860*, 1688-1709.
- (25) Williams, J. P.; Grabenauer, M.; Holland, R. J.; Carpenter, C. J.; Wormald, M. R.; Giles, K.; Harvey, D. J.; Bateman, R. H.; Scrivens, J. H.; Bowers, M. T. *Int. J. Mass Spectrom.* **2010**, *298*, 119-127.
- (26) Li, H.; Giles, K.; Bendiak, B.; Kaplan, K.; Siems, W. F.; Hill, H. H. *Anal. Chem.* **2012**, *84*, 3231-3239.
- (27) Li, H. L.; Bendiak, B.; Siems, W. F.; Gang, D. R.; Hill, H. H. *Rapid Commun. Mass Spectrom.* **2013**, *27*, 2699-2709.
- (28) Gaye, M. M.; Kurulugama, R.; Clemmer, D. E. *Analyst* **2015**, *140*, 6922-6932.
- (29) Huang, Y.; Dodds, E. D. *Anal. Chem.* **2015**, *87*, 5664-5668.
- (30) Guile, G. R.; Harvey, D. J.; O'Donnell, N.; Powell, A. K.; Hunter, A. P.; Zamze, S.; Fernandes, D. L.; Dwek, R. A.; Wing, D. R. *Eur. J. Biochem.* **1998**, *258*, 623-656.
- (31) Hernandez, H.; Robinson, C. V. *Nat. Protoc.* **2007**, *2*, 715-726.
- (32) Hofmann, J.; Struwe, W. B.; Scarff, C. A.; Scrivens, J. H.; Harvey, D. J.; Pagel, K. *Anal. Chem.* **2014**, *86*, 10789-10795.
- (33) Thalassinou, K.; Grabenauer, M.; Slade, S. E.; Hilton, G. R.; Bowers, M. T.; Scrivens, J. H. *Anal. Chem.* **2009**, *81*, 248-254.

- (34) Struwe, W. B.; Pagel, K.; Benesch, J. L. P.; Harvey, D. J.; Campbell, M. P. *Glycoconj. J.* **2016**, *33*, 399-404.
- (35) Struwe, W. B.; Agravat, S.; Aoki-Kinoshita, K. F.; Campbell, M. P.; Costello, C. E.; Dell, A.; Ten, F.; Haslam, S. M.; Karlsson, N. G.; Khoo, K. H.; Kolarich, D.; Liu, Y.; McBride, R.; Novotny, M. V.; Packer, N. H.; Paulson, J. C.; Rapp, E.; Ranzinger, R.; Rudd, P. M.; Smith, D. F.; Tiemeyer, M.; Wells, L.; York, W. S.; Zaia, J.; Kettner, C. *Glycobiology* **2016**, *26*, 907-910.
- (36) Kolarich, D.; Rapp, E.; Struwe, W. B.; Haslam, S. M.; Zaia, J.; McBride, R.; Agravat, S.; Campbell, M. P.; Kato, M.; Ranzinger, R.; Kettner, C.; York, W. S. *Molecular & Cellular Proteomics* **2013**, *12*, 991-995.
- (37) Harvey, D. J.; Merry, A. H.; Royle, L.; Campbell, M. P.; Dwek, R. A.; Rudd, P. M. *Proteomics* **2009**, *9*, 3796-3801.
- (38) Pagel, K.; Harvey, D. J. *Anal. Chem.* **2013**, *85*, 5138-5145.
- (39) Gelb, A. S.; Jarratt, R. E.; Huang, Y.; Dodds, E. D. *Anal. Chem.* **2014**, *86*, 11396-11402.
- (40) Penn, S. G.; Cancilla, M. T.; Lebrilla, C. B. *Anal. Chem.* **1996**, *68*, 2331-2339.
- (41) Albertolle, M. E.; Hassis, M. E.; Ng, C. J.; Cuison, S.; Williams, K.; Prakobphol, A.; Dykstra, A. B.; Hall, S. C.; Niles, R. K.; Ewa Witkowska, H.; Fisher, S. J. *Clin. Proteomics* **2015**, *12*, 29.
- (42) Burford-Mason, A. P.; Weber, J. C.; Willoughby, J. M. *J. Med. Vet. Mycol.* **1988**, *26*, 49-56.
- (43) Shin, E. S.; Chung, S. C.; Kim, Y. K.; Lee, S. W.; Kho, H. S. *Oral. Surg. Oral. Med. O.* **2003**, *96*, 48-53.
- (44) Guttman, M.; Lee, K. K. *Anal. Chem.* **2016**, *88*, 5212-5217.
- (45) Struwe, W. B.; Benesch, J. L.; Harvey, D. J.; Pagel, K. *Analyst* **2015**, *140*, 6799-6803.
- (46) Plasencia, M. D.; Isailovic, D.; Merenbloom, S. I.; Mechref, Y.; Novotny, M. V.; Clemmer, D. E. *J. Am. Soc. Mass Spectrom.* **2010**, *21*, 191-191.
- (47) Harvey, D. J. *J. Mass Spectrom.* **2000**, *35*, 1178-1190.

Abstract Graphic

